

## A transmission electron microscopy study of ferroelectric domains in a modified lead zirconate titanate ceramic

This article has been downloaded from IOPscience. Please scroll down to see the full text article.

1993 J. Phys.: Condens. Matter 5 5037

(<http://iopscience.iop.org/0953-8984/5/28/018>)

View [the table of contents for this issue](#), or go to the [journal homepage](#) for more

Download details:

IP Address: 171.66.16.159

The article was downloaded on 12/05/2010 at 14:12

Please note that [terms and conditions apply](#).

## A transmission electron microscopy study of ferroelectric domains in a modified lead zirconate titanate ceramic

Huilin Li††, Yuanwei Zhang††, Huamin Zou†† and Renhui Wang††

† Department of Physics, Wuhan University, 430072 Wuhan, People's Republic of China

†† Beijing Laboratory of Electron Microscopy, Chinese Academy of Sciences, 100080 Beijing, People's Republic of China

Received 21 December 1992, in final form 18 March 1993

**Abstract.** Microstructures of a modified PZT piezoelectric ceramic  $\text{Pb}(\text{Mg}_{1/3}\text{Nb}_{2/3})_A(\text{Mn}_{1/3}\text{Nb}_{2/3})_B\text{Zr}_C\text{Ti}_D\text{O}_3$  with  $A = 0.059$ ,  $B = 0.066$ ,  $C = 0.459$  and  $D = 0.416$  were investigated using transmission electron microscopy. Labyrinthic domain configurations were observed. *In situ* observations during heating were carried out in an electron microscope. The effect of electron beam irradiation on the ferroelectric-to-paraelectric phase transition was studied. An essentially one-dimensional array of microdomains and a vein configuration of microdomains were observed in the modified PZT piezoelectric ceramic specimen.

### 1. Introduction

A modified PZT piezoelectric ceramic  $\text{Pb}(\text{Mg}_{1/3}\text{Nb}_{2/3})_A(\text{Mn}_{1/3}\text{Nb}_{2/3})_B\text{Zr}_C\text{Ti}_D\text{O}_3$  ( $A = 0.059$ ,  $B = 0.066$ ,  $C = 0.459$  and  $D = 0.416$ ), developed recently at Hubei University, exhibits both stable temperature characteristics and excellent piezoelectric performance and thus is very suitable for fabricating piezoelectric ceramic transformers [1]. By varying the composition of the material, it is found that the transition position at which the slope of the curve of maximum variation in resonance frequency  $f_r$  versus temperature  $T$  changes from positive to negative depends not only on the Zr-to-Ti ratio but also on the values of  $A$  and  $B$ . These ceramics were referred to as PMMN quaternary system ceramics in [1]. The maximum output power of the transformer made with one piece of this modified PZT piezoelectric ceramic with dimensions  $100 \text{ mm} \times 25 \text{ mm} \times 3.6 \text{ mm}$  may reach 65 W, which is much larger than the values that piezoelectric ceramic transformers made of other materials, e.g. the ternary ceramics PCM and PSM, can give. This stimulated our interest in studying the microstructure of this material.

The ferroelectric domains in the perovskite-type oxides  $\text{BaTiO}_3$ ,  $\text{PbTiO}_3$  and  $\text{KNbO}_3$  have been studied by Tanaka and co-workers [2, 3]. The  $90^\circ$  domain configurations were described as two types: the plate-like  $a$ - $a$  domains and the wedge-like  $a$ - $c$  domains [2, 3]. The  $90^\circ$  domains lose their contrast when the diffraction vector  $g$  is perpendicular to the domain boundaries in the case of  $a$ - $a$  domains, while they lose their contrast when  $g$  is parallel to the domain boundaries in the case of  $a$ - $c$  domains. If only the crystallographic lattice is taken into account, the  $90^\circ$  domains are simply twins. The diffraction contrast of  $180^\circ$  domains was observed in bright-field images as well as in dark-field images. The origin of the contrast between  $180^\circ$  domains has been interpreted by Gevers *et al* [4], Tanaka and Honjo [2] and Tanaka [5]. At a temperature just below the paraelectric-to-ferroelectric phase transition point, microdomains were observed in  $\text{BaTiO}_3$  [6, 7] and

KNbO<sub>3</sub> [7]. The microdomains often appear as dots of contrast and wavy stripes with ill defined orientation and connectivity. The periodicity of approximately equal areas of light and dark contrast is about several hundred ångströms depending on the thickness of the TEM specimen. It has been proposed that the microdomains may be related to an intermediate structure between the paraelectric and ferroelectric phases [6, 7]. The TEM observations of microstructures at the morphotropic phase boundary of the PbTiO<sub>3</sub>-PbZrO<sub>3</sub> system showed that the domain structures of tetragonal and rhombohedral phases were similar and had plate-like configurations [8, 9]. TEM observations of tin-modified PZT ceramic also showed plate-like domain configurations [10]. The hot-pressed ceramic Pb(Zr<sub>0.58</sub>Fe<sub>0.20</sub>Nb<sub>0.20</sub>Ti<sub>0.02</sub>)<sub>0.995</sub>U<sub>0.005</sub>O<sub>3</sub> with rhombohedral symmetry below the transition temperature has been reported to have fine lamellar domains and zigzag domain boundaries [11]. Superlattice reflections have been found in the diffraction patterns of lead-based perovskites including PMN [12-14], PIN [14], PST [14], PLZT [14], Pb(Zr<sub>0.58</sub>Fe<sub>0.20</sub>Nb<sub>0.20</sub>Ti<sub>0.02</sub>)<sub>0.995</sub>U<sub>0.005</sub>O<sub>3</sub> [11, 14] and 95/5 PZT [15].

The domain configurations depend on extrinsic factors as well as intrinsic factors such as the jump in depolarizing field and the jump in spontaneous strain [16]. Since the modified PZT piezoelectric ceramic possesses some different properties from PZT, BaTiO<sub>3</sub>, etc, it is worth studying the domain structures of the material. In the present paper, we shall report our electron microscopy observations of the domain structures of the modified PZT piezoelectric ceramic, which shows some characteristics different from those reported so far, and the effects of electron beam irradiation on the domain structures.

## 2. Experimental details

Thin plates were cut from the modified PZT piezoelectric ceramic provided kindly by Professor A X Kuang in the Department of Physics, Hubei University. The chemical composition is



with  $A = 0.059$ ,  $B = 0.066$ ,  $C = 0.459$  and  $D = 0.416$ . Thin foils for TEM observation were thinned first by mechanical grinding and then by Ar ion milling. When the specimen was directly exposed to electron beam irradiation, considerable radiolysis took place. The originally large grains with an average diameter of 1.5  $\mu\text{m}$  became amorphous or very fine grains with a diameter of about 0.03  $\mu\text{m}$  on average. For studying the domain structures, the specimens were coated with carbon films. The TEM experiments were carried out on JEOL JEM 100CX(II) and Philips CM12 transmission electron microscopes operated at an accelerating voltage of 120 kV.

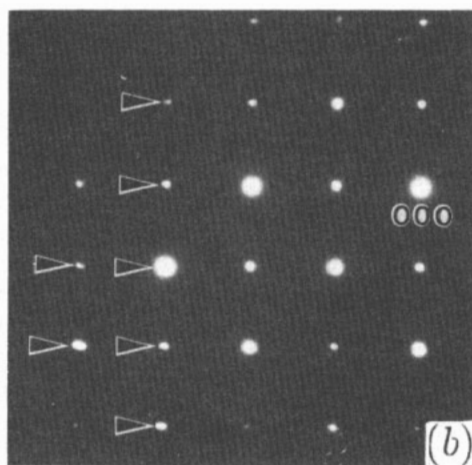
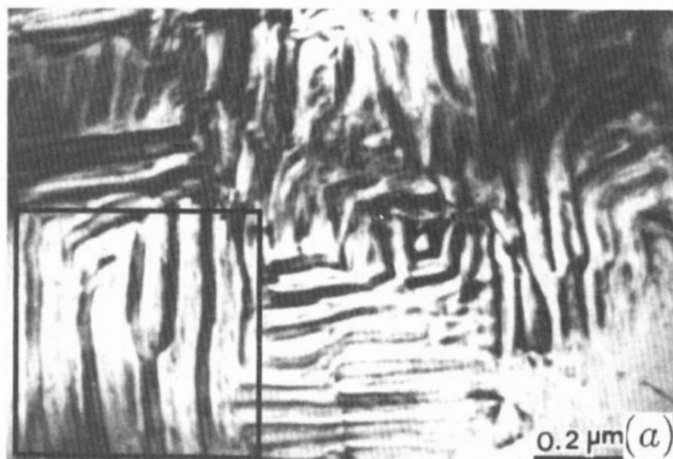
## 3. Results and discussion

### 3.1. Domain configurations

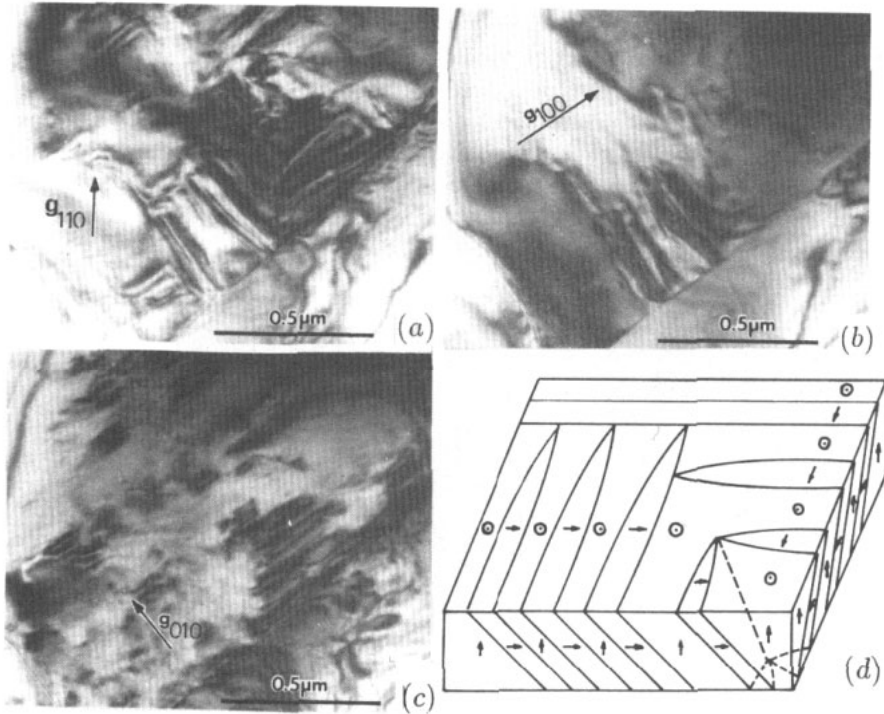
X-ray diffraction structure analysis at room temperature shows that the modified PZT piezoelectric ceramic studied in the present work is a tetragonal phase with  $a = 0.4051$  nm and  $c = 0.4135$  nm.

Figure 1(a) shows a labyrinthic domain configuration with the [001]<sub>p</sub> (where the subscript p indicates pseudo-cubic) direction of the crystal parallel to the incident electron

beam. The domain boundaries are approximately parallel to  $[100]_p$  or  $[010]_p$ . Figure 1(b), the diffraction pattern taken from the set of parallel stripes in the rectangle in figure 1(a), shows that diffraction spots are elongated in a direction, say  $[100]_p$ , as indicated by arrows, while they are round in the direction perpendicular to that direction, say  $[010]_p$ . This means that the crystallographic plane spacings of the two sets of domains are different in the direction of  $[100]_p$ , i.e. the so-called *a* domains have their *c* axis parallel to  $[100]_p$ , and the so-called *c* domains have their *a* or *b* axis parallel to  $[100]_p$ . This feature of the diffraction pattern implies that the domain boundaries are *a*-*c* 90° domain walls.



**Figure 1.** (a) Labyrinthine domain configuration taken with the electron beam parallel to the  $[001]_p$  axis; (b) diffraction pattern taken from the area in the rectangle in (a). The split diffraction spots are indicated with arrows.



**Figure 2.** (a)–(c) Bright-field images taken under (a) the  $hh0_p$  systematic reflection condition, (b) the  $h00_p$  systematic reflection condition and (c) the  $0k0_p$  systematic reflection condition. (d) The schematic labyrinthine domain configuration.

Diffraction contrast experiments confirm this conclusion. Figure 2(a), which was taken with the  $hh0_p$  systematic reflection condition, shows the two perpendicular sets of stripes parallel to  $[100]_p$  and  $[010]_p$  directions, respectively. The stripes along the  $[100]_p$  direction lose their contrast at the  $h00_p$  systematic reflection setting, as shown in figure 2(b), and the stripes along the  $[010]_p$  direction lose their contrast in the  $0k0_p$  systematic row diffraction condition, as shown in figure 2(c). Two points can be drawn from these observations. First, the contrast shown in the labyrinthine domain configuration is due to the diffraction contrast effect. Second, according to the diffraction contrast theory, the displacement vectors are perpendicular to  $[010]_p^*$  for the set of domains appearing in figure 2(b), and to  $[100]_p^*$  for domains in contrast in figure 2(c). The schematic diagram of the labyrinthine domain configuration may be drawn as figure 2(d). This labyrinthine domain configuration has not been reported in the literature for other materials so far to the knowledge of the present authors.

### 3.2. Irradiation effect

The domain structure of the modified PZT piezoelectric ceramic is very sensitive to the electron beam irradiation, although the TEM specimen is carbon film coated. Figure 3(a) was taken by using spot size '5' in the CM12 microscope and an exposure time of 50 s chosen by the automatic exposure controller. Figure 3(b) was taken with spot size '2' and an exposure time of 5 s. It is seen that the contrast of the domain walls disappeared under

the illumination of the stronger electron beam. The experiments also showed that the lost domain contrast reappeared only a few seconds later after the electron beam intensity was reduced.

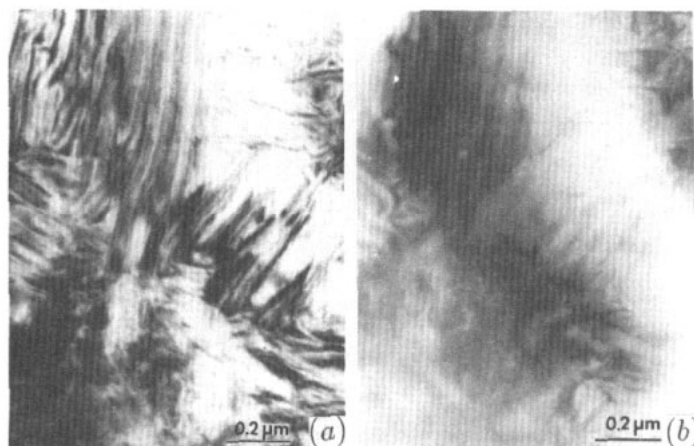


**Figure 3.** (a) Bright-field image taken with spot size '5' and an exposure time of 50 s chosen by the automatic exposure time controller. (b) Bright-field image taken with spot size '2' and an exposure time of 5 s chosen by the automatic exposure timer.

To explain the phenomenon under electron beam irradiation, the first point considered is the electron-beam-heating effect. As discussed by Steeds [17], a temperature rise of 50 °C can be detected for metals and alloys; however, a temperature rise of more than 300 °C could be produced in the illuminated area of LiTaO<sub>3</sub> for large beam currents because of the poor thermal conductivity of the material. The thermal conductivity of amorphous carbon solid is 0.0150 W cm<sup>-1</sup> K<sup>-1</sup> at 273.2 K and 0.0182 W cm<sup>-1</sup> K<sup>-1</sup> at 373.2 K [18]. Because both the ceramic and the coated amorphous carbon film are poor thermal conductors, the temperature of the area illuminated with a strong electron beam may well rise to near the phase transition point.

Also, microdomains were observed in the specimen of the modified PZT piezoelectric ceramic, as shown in figure 4. The aligned microdomains lying on (110)<sub>p</sub> with periodicity varying from 10 to 30 nm can be seen in regions A and B, while tweed microdomain structures are seen in region C. The microdomain alignment can be induced by a build-up of charge on the specimen in the electron beam of the microscope [19]. The microdomains are usually observed at a temperature several degrees Celsius lower than the phase transition point in the cases of BaTiO<sub>3</sub> [6, 7] and KNbO<sub>3</sub> [7]. The observation of microdomains indicates that a temperature rise and a build-up of charge have taken place.

In order to obtain full understanding of the effect of electron beam irradiation on the domain structures, *in situ* observations during heating were carried out with a heating specimen stage in the JEM-100CX(II). As the temperature increased to about 320 °C, the domain contrast quickly disappeared, as shown in figures 5(a) and 5(b). When the temperature decreased, the domain contrast appeared again, as shown in figure 5(c).

From our experience in studying the phase transformation of metals, the temperature value measured with the thermocouple of the heating stage is within an error range of ±10 °C from the actual temperature in the specimen area under observation in the case of metallic

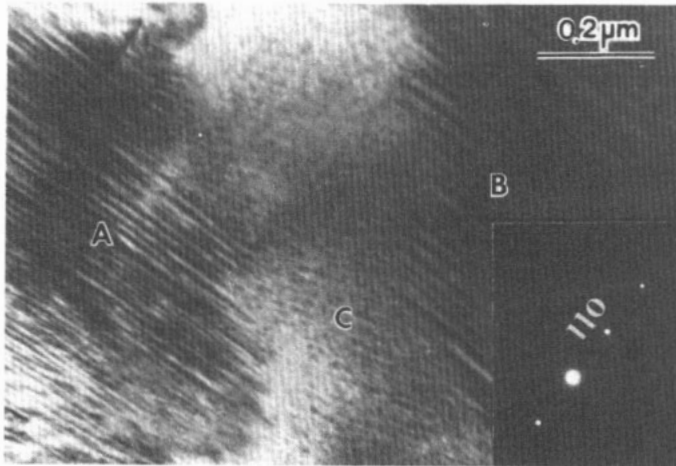


**Figure 4.** Microdomains seen in the sample suffered several strong- and weak-electron-beam-illumination cycling processes. The quasi-one-dimensional array of microdomains lying on the  $(110)_p$  plane can be seen in regions A and B. The tweed configuration of microdomains is seen in region C. The corresponding diffraction pattern is shown in the inset.

samples and of the temperature range around 300 °C. However, the deviation of the measured temperature from the actual temperature depends on the heat conductivity of the specimen material, the rate of electron energy dissipation and the heat radiation conditions. Also the phase transition temperature of the sample may vary with the thickness of the specimen area under observation. It is, therefore, difficult to conclude the actual temperature from such measurements [20]. The ferroelectric-to-paraelectric phase transition temperature  $T_c$  measured in terms of the dependence of dielectric constant on temperature is about 346 °C. The Curie temperature of a thin-foil TEM specimen of the ceramic may be different from that of the bulk material [21]. The TEM specimen was coated with a carbon film which usually prevented the build-up of charge. Hence, the loss of domain contrast under high-intensity electron beam illumination may be mainly because the heating effect caused by inelastic scattering of the incident electrons within the specimen makes the ferroelectric-to-paraelectric phase transition possible in the case without an external heating source.

An attempt to observe the superlattice reflections in electron diffraction patterns has been made using a liquid-nitrogen-cooled stage and a long exposure time. However, no superlattice reflections were observed in the diffraction patterns for the modified PZT piezoelectric ceramic (see figure 1(b)). An x-ray diffraction experiment carried out on the ceramic showed that the superlattice reflection  $(\frac{3}{2}, \frac{3}{2}, 0)$  occurred as a weak peak at  $2\theta = 47.6^\circ$  (Cu  $K\alpha$ ). These observations imply that the superstructure in the modified PZT piezoelectric ceramic is very unstable under electron beam irradiation compared with those in the ferroelectric relaxor materials.

#### 4. Summary

The microstructure of the modified PZT piezoelectric ceramic has been studied with transmission electron microscopy.

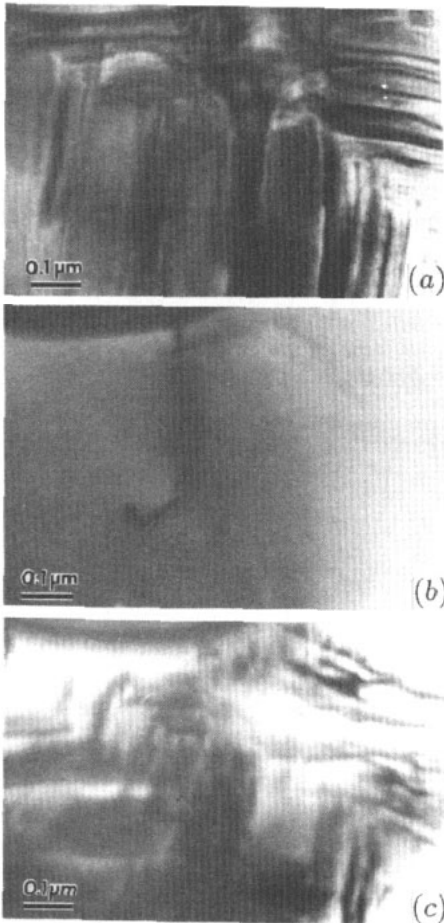


**Figure 5.** *In situ* observation during heating: (a) at room temperature, domains are clearly seen in the picture; (b) at 320°C, no domain contrast can be seen; (c) the domains reappear when the sample is cooled.

(1) A labyrinthine domain structure with domains of  $a$ - $c$  90° type was observed for the first time.

(2) Both a quasi-one-dimensional array of microdomains and a vein microdomain structure configuration were observed in the modified PZT piezoelectric ceramic.

(3) The high-intensity electron beam illumination may induce the ferroelectric-to-paraelectric phase transition due to the electron-beam-heating effect.

## References

- [1] Kuang A and Zhou T 1990 *Ferroelectrics* **101** 29
- [2] Tanaka M and Honjo G 1964 *J. Phys. Soc. Japan* **19** 954
- [3] Tanaka M, Yatsuhashi T and Honjo G 1970 *J. Phys. Soc. Japan Suppl.* **28** 386
- [4] Gevers R, Blank H and Amelinckx A 1966 *Phys. Status Solidi* **13** 449
- [5] Tanaka M 1975 *Acta Crystallogr. A* **31** 59
- [6] Bursill L A and Peng Juling 1984 *Nature* **311** 550
- [7] Cheng J, Fan C, Li Q and Feng D 1988 *J. Phys. C: Solid State Phys.* **21** 2255
- [8] Yamamoto T, Ohazaki K, Dass M L and Thomas G 1988 *Ferroelectrics* **81** 331
- [9] Lucuta P G 1989 *J. Am. Ceram. Soc.* **72** 933



- [10] Hardiman B, Zeyfang R and Reeves C 1973 *J. Appl. Phys.* **44** 5266
- [11] Randall C A, Barber D J and Whatmore R W 1985 *Electron Microscopy and Analysis 1985 (Inst. Phys. Conf. Ser. 78)* (Bristol: Institute of Physics) p 531
- [12] Chen J, Chan H M and Harmer M P 1989 *J. Am. Ceram. Soc.* **72** 593
- [13] Hilton A D, Randall C A, Barber D J and Shroud T R 1989 *Ferroelectrics* **93** 379
- [14] Randall C, Barber D, Whatmore R and Groves P 1987 *Ferroelectrics* **76** 277
- [15] Chang Y J 1982 *Appl. Phys. A* **29** 237
- [16] Fesenko E G, Gavril'yachenko V G, Semenchov A F and Yufatova S M 1985 *Ferroelectrics* **63** 289
- [17] Steeds J W 1979 *Introduction to Analytical Electron Microscopy* ed J J Wren, J I Goldstein and D C Joy (New York: Plenum) ch 15, p 387
- [18] Weast R C (ed) 1974 *Handbook of Chemistry and Physics* 55th edn (Boca Raton, FL: Chemical Rubber Company) p E12
- [19] Randall C, Barber D, Whatmore R and Groves P 1987 *Ferroelectrics* **76** 311
- [20] Urban K, Moser N and Kronmuller H 1985 *Phys. Status Solidi a* **91** 411
- [21] Wang C L, Zhong W L and Zhang P L 1992 *J. Phys.: Condens. Matter* **3** 4743